

Exploring the Hubble Tension and Spatial Curvature from the Ages of Old Astrophysical Objects

JUN-JIE WEI^{1,2,3} AND FULVIO MELIA⁴

¹*Purple Mountain Observatory, Chinese Academy of Sciences, Nanjing 210033, China*

²*Guangxi Key Laboratory for Relativistic Astrophysics, Nanning 530004, China*

³*School of Astronomy and Space Sciences, University of Science and Technology of China, Hefei 230026, China*

⁴*Department of Physics, The Applied Math Program, and Department of Astronomy, The University of Arizona, Tucson, AZ 85721, USA*

ABSTRACT

We use the age measurements of 114 old astrophysical objects (OAO) in the redshift range $0 \lesssim z \lesssim 8$ to explore the Hubble tension. The age of the Universe at any z is inversely proportional to the Hubble constant, H_0 , so requiring the Universe to be older than the OAO it contains at any z will lead to an upper limit on H_0 . Assuming flat Λ CDM and setting a Gaussian prior on the matter density parameter $\Omega_m = 0.315 \pm 0.007$ informed by *Planck*, we obtain a 95% confidence-level upper limit of $H_0 < 70.6 \text{ km s}^{-1} \text{ Mpc}^{-1}$, representing a 2σ tension with the measurement using the local distance ladder. We find, however, that the inferred upper limit on H_0 depends quite sensitively on the prior for Ω_m , and the Hubble tension between early-time and local measurements of H_0 may be due in part to the inference of both Ω_m and H_0 in *Planck*, while the local measurement uses only H_0 . The age-redshift data may also be used for cosmological model comparisons. We find that the $R_h = ct$ universe accounts well for the data, with a reasonable upper limit on H_0 , while Einstein-de Sitter fails to pass the cosmic-age test. Finally, we present a model-independent estimate of the spatial curvature using the ages of 61 galaxies and the luminosity distances of 1,048 Pantheon Type Ia supernovae. This analysis suggests that the geometry of the Universe is marginally consistent with spatial flatness at a confidence level of 1.6σ , characterized as $\Omega_k = 0.43^{+0.27}_{-0.27}$.

Keywords: Cosmological parameters (339) — Cosmological models (337) — Hubble constant (758) — Galaxy ages (576) — Quasars (1319) — Type Ia supernova (1728)

1. INTRODUCTION

Since the first discovery of the expansion of the Universe more than 90 years ago (Lemaître 1927; Hubble 1929), the Hubble constant H_0 characterizing its current expansion rate has been of great interest to astronomers. In the last decade, however, a significant mismatch has emerged between several early-time and local measurements of H_0 (see Verde et al. 2019; Di Valentino et al. 2021 for recent reviews). The latest value of H_0 ($= 73.2 \pm 1.3 \text{ km s}^{-1} \text{ Mpc}^{-1}$; Riess et al. 2021) measured from local Type Ia supernovae (SNe Ia), calibrated by the Cepheid distance ladder, is in 4.2σ tension with that inferred from *Planck* cosmic microwave background (CMB) observations interpreted in the context of the standard Λ CDM model ($H_0 = 67.4 \pm 0.5 \text{ km s}^{-1} \text{ Mpc}^{-1}$; Planck Collaboration et al. 2020). If the unknown system-

atics cannot be responsible for the discrepancy, the Hubble tension may imply new physics beyond Λ CDM (Melia 2020; Vagnozzi 2020).

In order to resolve the Hubble tension, more independent methods of measuring H_0 are required. For example, the age of the oldest stellar populations in our galaxy can provide an independent local determination of H_0 (Trenti et al. 2015; Jimenez et al. 2019; Valcin et al. 2020; Bernal et al. 2021; Boylan-Kolchin & Weisz 2021). But most age measurements use objects at higher redshifts, which can also constrain other cosmological parameters (e.g., Bolte & Hogan 1995; Krauss & Turner 1995; Dunlop et al. 1996; Alcaniz & Lima 1999; Lima & Alcaniz 2000; Jimenez & Loeb 2002; Jimenez et al. 2003; Capozziello et al. 2004; Friaça et al. 2005; Simon et al. 2005; Jain & Dev 2006; Pires et al. 2006; Dantas et al. 2007, 2009, 2011; Samushia et al. 2010; Bengaly et al. 2014; Wei et al. 2015; Rana et al. 2017; Nunes & Pacucci 2020; Vagnozzi et al. 2021a). Very recently, Vagnozzi et al. (2021b) used the age estimates of high-redshift (up to $z \sim 8$)

old astrophysical objects (OAO) to derive an upper limit on H_0 by requiring that all OAO at any z must be younger than the age of the Universe at that redshift. Their study shed some light on the ingredients needed to resolve the Hubble tension, but to constrain H_0 in this manner, one has to assume a background cosmology. Assuming the validity of Λ CDM at late times, Vagnozzi et al. (2021b) found a 95% confidence-level upper limit of $H_0 < 73.2 \text{ km s}^{-1} \text{ Mpc}^{-1}$, marginally consistent with that measured using the local distance ladder.

Of direct relevance to the principal aim of this paper is the fact that, unlike the cosmic distance ladder methods that rely on the distances of primary or secondary indicators, the age measurements of distant objects are independent of each other. The age-redshift relationship of high- z OAO may therefore provide a whole new perspective on one of the most frontier issues in modern cosmology, i.e., the spatial curvature of the Universe. Knowing whether the Universe is open, closed, or flat is crucial for a complete understanding of its evolution and the nature of dark energy (Ichikawa et al. 2006; Clarkson et al. 2007; Gong & Wang 2007; Virey et al. 2008). A significant deviation from zero spatial curvature would have far-reaching consequences for the inflationary paradigm and its underlying physics (Eisenstein et al. 2005; Tegmark et al. 2006; Wright 2007; Zhao et al. 2007; Melia 2020).

Although a spatially flat universe ($\Omega_k = 0$) is strongly favored by most of the current cosmic probes, especially by the *Planck* 2018 CMB observations (Planck Collaboration et al. 2020),¹ these curvature determinations are based on the pre-assumption of a particular cosmological model (e.g., Λ CDM). But there is a strong degeneracy between the curvature parameter and the dark-energy equation of state, so it would be better to measure the purely geometric quantity Ω_k from the data using a model-independent method. A non-exhaustive set of references attempting to constrain the value of Ω_k in a model-independent way includes Bernstein (2006), Clarkson et al. (2007), Shafieloo & Clarkson (2010), Li et al. (2014, 2016, 2018a,b, 2019a,b, 2020), Sapone et al. (2014), Räsänen et al. (2015), Cai et al. (2016), Yu & Wang (2016), L’Huillier & Shafieloo (2017), Liao et al. (2017), Rana et al. (2017), Wang et al. (2017, 2020, 2021b), Wei & Wu (2017), Xia et al. (2017), Denissenya et al. (2018), Wei (2018), Witzemann et al. (2018), Yu et al. (2018), Collett et al. (2019), Cao et al. (2019a,b, 2021), Liao (2019), Ruan et al. (2019), Qi et al. (2019a,b), Liu et al. (2020), Wei & Melia (2020a,b), Zhou & Li (2020), Dhawan et al. (2021),

Jesus et al. (2021), Vagnozzi et al. (2021a), Yang & Gong (2021), and Zheng et al. (2021).

In this paper, we broaden the base of support for the age measurements of high- z OAO by demonstrating their usefulness in testing the late-time expansion history and arbitrating the Hubble tension in different cosmological models. Further, we propose a new model-independent method of determining the spatial curvature by combining the OAO age- z data with SNe Ia luminosity distances. Using a polynomial fitting technique, we reconstruct a continuous age- z function representing the discrete age measurements of OAO without the pre-assumption of any specific cosmological model. The time-redshift derivative dt/dz can then be approximately obtained by differentiating the age- z function. Then, dt/dz can be transformed into the curvature-dependent luminosity distance $D_L(\Omega_k; z)$ according to the geometric relation derived from the Friedmann-Lemaître-Robertson-Walker (FLRW) metric. Finally, by carrying out the joint maximum likelihood analysis on the polynomial fitting and the observed differences between $D_L(\Omega_k; z)$ and the curvature-independent luminosity distances inferred from SNe Ia, one can simultaneously constrain the curvature parameter Ω_k , the polynomial coefficients, and the SN nuisance parameters in a model-independent way.

The paper is arranged as follows. In § 2, we briefly describe the age-redshift test, and then constrain H_0 in different cosmological models. In § 3, we introduce the methodology of measuring Ω_k using OAO age- z and SN Ia data, and then present the results of our analysis. We summarize our main conclusions in § 4.

2. EXPLORATION ON THE HUBBLE TENSION

2.1. The Age-redshift Test

The theoretical age of the Universe at redshift z is given as

$$t(z) = \int_z^\infty \frac{dz'}{(1+z')H(z', \theta)}, \quad (1)$$

where $H(z, \theta)$ is the Hubble parameter and θ stands for the parameters of the specific cosmological model. All of our analysis in this paper is based on this expression, which is derived from the FLRW metric. In so doing, we restrict our attention to the spacetime predicted in the context of general relativity only, though we shall consider possible model variations consistent with this constraint as prescribed via the choice of stress-energy tensor in Einstein’s equations, which are characterized by the specific model parameters θ .

The age $t_{\text{obj},i}$ of an object (e.g., a passive galaxy or quasar) at redshift z_i is defined as the difference between the age of the Universe at z_i and that when the object was formed at redshift z_f . Given that no object was born at the Big Bang ($z_f \rightarrow \infty$), the age of the Universe at any redshift should always be greater than or equal to the age of the oldest astro-

¹ Some recent studies show that the *Planck* 2015 CMB anisotropy data support a mildly closed Universe (see Park & Ratra 2019a,b and references therein).

physical object (OAO) at the same redshift, i.e., $t(z_i) \geq t_{\text{obj},i}$. The difference between $t(z_i)$ and $t_{\text{obj},i}$, which we denote by τ_{inc} , represents the ‘incubation’ time, or delay factor, and accounts for the amount of time elapsed since the Big Bang to the formation of the object.

Equation (1) shows that the age of the Universe at any given redshift is inversely proportional to the Hubble constant $H_0 \equiv H(z=0)$. An upper limit on H_0 can therefore be obtained by requiring that the Universe be at least as old as the oldest objects at the corresponding redshifts (Vagnozzi et al. 2021b). If the value of H_0 is too high, then we are in an awkward position that the Universe is younger than the oldest objects it contains at a given redshift. In Equation (1), $t(z)$ receives most of its contribution at late times ($z \leq 10$), and is scarcely sensitive to pre-recombination physics. Therefore, consistency between the high- z upper limits on H_0 and the local H_0 measurements offers a stringent test of late-time and/or local new physics, potentially suggesting the necessity for the latter to operate together with early-time new physics to completely address the Hubble tension (Krishnan et al. 2020, 2021a,b; Dainotti et al. 2021; Jedamzik et al. 2021; Lin et al. 2021; Vagnozzi 2021; Vagnozzi et al. 2021b).

Using a combination of galaxies and high- z quasars, Vagnozzi et al. (2021b) constructed an age-redshift diagram of OAO up to $z \sim 8$. Most of their galaxy data come from the Cosmic Assembly Near-infrared Deep Extragalactic Legacy Survey (CANDELS) observing program (Grogin et al. 2011), and the remaining galaxy data are from the observations of 32 old passive galaxies in the redshift range $0.117 \leq z \leq 1.845$ (Simon et al. 2005). For high- z quasars, they considered the following observations: 7,446 quasars from SDSS DR7 in the range $3 \leq z \leq 5$ (Shen et al. 2011), 50 quasars detected by the GNIRS spectrograph in the range $5.5 \leq z \leq 6.5$ (Shen et al. 2019), 15 quasars detected by Pan-STARRS1 in the range $6.5 \leq z \leq 7.0$ (Mazzucchelli et al. 2017), and 9 of the most distant quasars ever discovered in the range $7.0 \leq z \leq 7.642$ (Mortlock et al. 2011; Bañados et al. 2018; Wang et al. 2018, 2021a; Matsuoka et al. 2019a,b; Yang et al. 2019, 2020). Basically, the ages of the CANDELS galaxies were estimated by fitting the photometric spectral energy distribution, whereas for the quasars a specific growth model of black hole seeds developed by Pacucci et al. (2017) was adopted. Applying severe quality cuts to these observations, and selecting only those objects which are among the oldest ones within each redshift bin, Vagnozzi et al. (2021b) compiled a final catalog of 114 OAO with reliable redshift and age measurements, in which 61 OAO are galaxies and the other 53 are quasars. We adopt this high- z OAO catalog covering the redshift range $0 < z < 8$ for our assessment of the H_0 limits. Figure 1 shows the age measurements as a function of red-

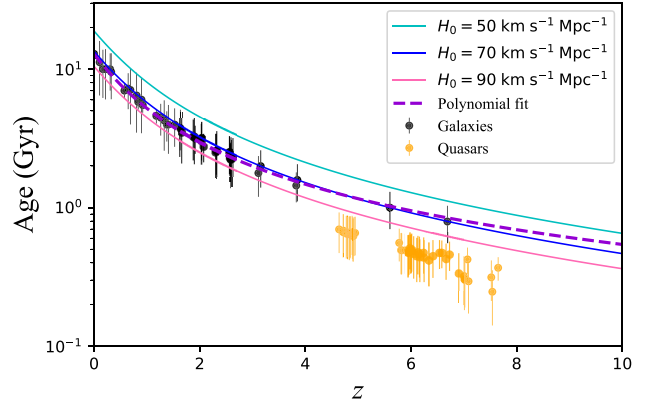


Figure 1. Age-redshift diagram for 114 OAO, including 61 galaxies (black points) and 53 quasars (orange points). The solid curves show the age of the Universe as a function of redshift in flat Λ CDM with a fixed $\Omega_m = 0.3$, but an adjustable H_0 . The violet dashed curve shows the inferred result when fitting solely the age-redshift data of the 61 galaxies using a third-order polynomial.

shift for these 114 OAO. In this plot, we also illustrate the dependence of the Universe’s age $t(z)$ (estimated using flat Λ CDM with a fixed matter density $\Omega_m = 0.3$) on the value of the Hubble constant H_0 .

2.2. Upper Limits on H_0

We are now in position to use the selected 114 age measurements of OAO as a function of redshift to derive upper limits on H_0 . Given the observed data \mathbf{D} (with the OAO ages at redshifts z_i being $t_{\text{obj},i} \pm \sigma_{t_{\text{obj},i}}$; see solid points in Figure 1) and some prior knowledge about the hypothetical models (for which the parameters are denoted by the vector θ), the posterior probability distributions of the free parameters can be modeled through the half-Gaussian (log-)likelihood (Vagnozzi et al. 2021b):

$$\ln \mathcal{L}(\theta | \mathbf{D}) = -\frac{1}{2} \sum_i^{114} \begin{cases} \Delta_i^2(\theta) / \sigma_{t_{\text{obj},i}}^2 & \text{if } \Delta_i(\theta) < 0 \\ 0 & \text{if } \Delta_i(\theta) \geq 0, \end{cases} \quad (2)$$

where $\Delta_i \equiv t(\theta, z_i) - t_{\text{obj},i}$ is defined as the age of the Universe minus the age of the i -th OAO at redshift z_i . The expression in Equation (2) is based on the fact that: *a*) since the Universe must not be younger than its oldest inhabitants, parameters for which the Universe is younger than the OAO (i.e., $\Delta_i(\theta) < 0$) are exponentially unlikely, and this means the more the Universe is younger than the OAO, the worse the fit; *b*) parameters for which the Universe is older than the OAO (i.e., $\Delta_i(\theta) \geq 0$) are equally likely, and cannot be distinguished solely on the basis of the OAO age.

To calculate model predictions for the age $t(z)$ in Equation (1), we need an expression for $H(z, \theta)$. As the cosmic expansion rate within the context of specifically selected

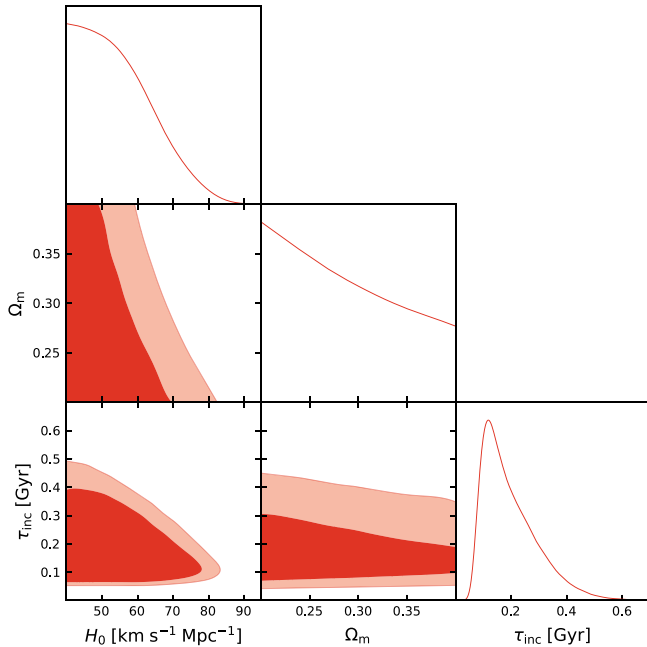


Figure 2. 1D and 2D marginalized posterior distributions with the $1-2\sigma$ contours for H_0 , Ω_m , and the incubation time τ_{inc} , using the 114 age-redshift data shown in Figure 1 and the same priors on H_0 , Ω_m , and τ_{inc} as Vagnozzi et al. (2021b).

models is significantly different, it is interesting to examine the upper limits on H_0 derived from the OAO ages using different background cosmologies. Here we discuss how these limits are obtained for Λ CDM, the Einstein-de Sitter universe, and the $R_h = ct$ universe.

- Λ CDM

In flat Λ CDM, the Hubble parameter is well approximated by

$$H^{\Lambda\text{CDM}}(z, \theta) = H_0 [\Omega_m(1+z)^3 + \Omega_\Lambda]^{1/2}, \quad (3)$$

where $\Omega_\Lambda = 1 - \Omega_m$ is the cosmological constant energy density. Note that we ignore the contribution from radiation, which is negligible compared to that of matter and dark energy in the late-time expansion history. The analysis of the OAO ages provides a valuable consistency test: if we trust the data, a disagreement between our upper limit on H_0 and the value measured from the local distance ladder may indicate new physics beyond Λ CDM, at least in the late-time expansion history.

For the basic Λ CDM model, the free parameters to be constrained are $\theta = \{H_0, \Omega_m\}$. We adopt the Python Markov chain Monte Carlo (MCMC) module, EMCEE (Foreman-Mackey et al. 2013), to explore the posterior probability distributions of these parameters. Note that Vagnozzi et al. (2021b) expressed Δ_i in Equation (2) as $\Delta_i \equiv t(\theta, z_i) - t_{\text{obj},i} - \tau_{\text{inc}}$, and modeled the incubation time

τ_{inc} as a prior distribution derived by Jimenez et al. (2019), based on the assumption that the formation redshift z_f for the oldest observed galaxies is $z_f > 11$. After marginalizing over H_0 , Ω_m , and z_f , this approach yields a prior peaked at $\tau_{\text{inc}} \approx 0.1 - 0.15$ Gyr, which Vagnozzi et al. (2021b) labeled as J19 and adopted its fitting function provided in Appendix G of Valcin et al. (2020).

For the quasars, Vagnozzi et al. (2021b) fixed $\tau_{\text{inc}} = t(z_f = 20)$, under the assumption that they were all seeded at redshift $z_f \sim 20$. In their baseline analysis, Vagnozzi et al. (2021b) set flat priors on $H_0 \in [40, 100]$ $\text{km s}^{-1} \text{Mpc}^{-1}$ and $\Omega_m \in [0.2, 0.4]$, the J19 prior on τ_{inc} for the galaxies, and fixed $\tau_{\text{inc}} = t(z_f = 20)$ for the quasars. To verify the reliability of our calculations, we have carried out a parallel analysis with the same priors on H_0 , Ω_m , and τ_{inc} to ensure that our results are consistent with each other. Figure 2 shows the joint $H_0 - \Omega_m - \tau_{\text{inc}}$ posterior distributions obtained from the baseline analysis suggested by Vagnozzi et al. (2021b). Our 95% confidence-level upper limit on the reduced Hubble constant $h_0 \equiv H_0 / (100 \text{ km s}^{-1} \text{Mpc}^{-1}) < 0.732$ (all quoted upper limits will hereafter be at the 95% confidence level) is the same as that obtained by Vagnozzi et al. (2021b). Our methodology can thus reliably incorporate the constraints of Vagnozzi et al. (2021b), producing results consistent with their analysis.

As one can see from Equations (1) and (2), however, the inclusion of τ_{inc} clearly results in a more stringent, less conservative limit on H_0 , depending on one's choice of the initial conditions. In addition, the derived τ_{inc} distribution from Jimenez et al. (2019) depends (though only weakly) on the assumed Λ CDM cosmology. In order to be as conservative as possible, and to provide the most reliable upper limits, we suggest to avoid introducing τ_{inc} in Equation (2). For the rest of this section, we shall therefore begin by conservatively constraining H_0 without the inclusion of this incubation time.

In our analysis, we choose wide flat priors for $H_0 \in [0, 150]$ $\text{km s}^{-1} \text{Mpc}^{-1}$ and $\Omega_m \in [0.2, 0.4]$. The 1D marginalized posterior distributions and 2D plots of the $1-2\sigma$ confidence regions for these two parameters, constrained by the 114 age-redshift data, are displayed in Figure 3 (red contours). These contours show that, whereas Ω_m is not as well constrained, we can set an upper limit on H_0 , whose 95% confidence-level value is $h_0 < 0.755$. This is roughly consistent with its latest local measurement ($h_0 = 0.732 \pm 0.013$; Riess et al. 2021). To explore the impact of a τ_{inc} prior, Vagnozzi et al. (2021b) also analyzed the data without its inclusion, i.e., by setting $\tau_{\text{inc}} = 0$ Gyr, finding in this case that $h_0 < 0.791$, which is somewhat incompatible with our result ($h_0 < 0.755$). The difference appears to be due to the fact that Vagnozzi et al. (2021b) set a narrower prior on $h_0 \in [0.4, 1]$, while we put $h_0 \in [0, 1.5]$. The relatively low values of H_0 are equally favored by the half-Gaussian likelihood (Eqn. 2).

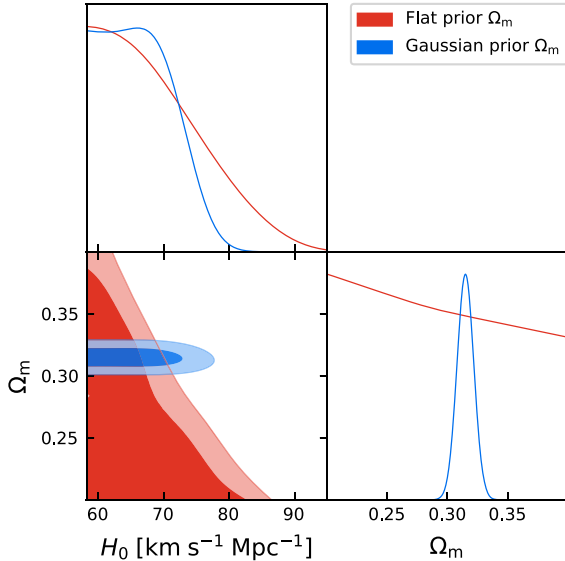


Figure 3. 1D and 2D marginalized posterior distributions with the $1-2\sigma$ contours for the parameters H_0 and Ω_m in flat Λ CDM, using the 114 age-redshift data shown in Figure 1. Different colored contours correspond to different priors on Ω_m : flat prior $\Omega_m \in [0.2, 0.4]$ (red contours) and Gaussian prior $\Omega_m = 0.315 \pm 0.007$ (blue contours).

If one insists on using Λ CDM as the background cosmology, the version that appears to be consistent with the majority of observations is spatially flat, with a scaled matter density $\Omega_m \approx 0.3$ (e.g., Aubourg et al. 2015; Scolnic et al. 2018; Planck Collaboration et al. 2020). Nevertheless, a peculiarity of the often made comparison between the measurements of H_0 at low and high redshifts in this model is that H_0 is constrained on its own for the former, but only in concert with other parameters, particularly Ω_m , for the latter.

Thus, to investigate how our results may be affected by the priors for these other concordance parameters, we sample the limits imposed on H_0 using alternate values of the matter density. First, we adopt the Gaussian prior $\Omega_m = 0.315 \pm 0.007$ from *Planck* (Planck Collaboration et al. 2020). The resulting constraints are shown as blue contours in Figure 3. In this case, the Ω_m posterior unsurprisingly follows its Gaussian prior, and h_0 is constrained to be $h_0 < 0.706$, representing a 2σ tension with its locally measured value. But it is important to note that it agrees with the *Planck* inference ($h_0 = 0.674 \pm 0.005$; Planck Collaboration et al. 2020). This is very interesting because, in this case, the outcomes for both H_0 and Ω_m are mutually consistent for both *Planck* and the OAO age-redshift data.

Next, we explore the impact of an Ω_m prior by fixing its value to be 0.1, 0.3, 0.5, 0.7, and 0.9, respectively. The outcome of each case is presented in Table 1. One can see that the inferred upper limit on H_0 does depend quite significantly

Table 1. The 95% confidence-level upper limits on H_0 with different Ω_m priors

Ω_m (fixed)	0.1	0.3	0.5	0.7	0.9
$H_0 / [\text{km s}^{-1} \text{Mpc}^{-1}]$	<112.4	<72.2	<56.6	<47.9	<42.4

on Ω_m . That is, some of the impact of adjusting H_0 for the fits is mitigated by corresponding changes to Ω_m . And since the local measurement of H_0 does not require Ω_m , while *Planck* uses both, the tension between the two measurements may be due in part to the use of Ω_m in the latter, but not the former.

- The $R_h = ct$ universe

The expansion rate in the $R_h = ct$ universe (Melia 2003, 2007, 2013; Melia & Shevchuk 2012; Wei et al. 2015; Melia 2020), is given as

$$H^{R_h=ct}(z, \theta) = H_0(1+z). \quad (4)$$

The $R_h = ct$ cosmology has only one free parameter, i.e., $\theta = \{H_0\}$. Here we also set a flat prior on $H_0 \in [0, 150] \text{ km s}^{-1} \text{Mpc}^{-1}$. The results of fitting the 114 age-redshift data with this cosmology are shown in the left panel of Figure 4. We find an upper limit of $h_0 < 0.861$ at the 95% confidence-level, in good agreement with the locally measured H_0 .

- Einstein-de Sitter

The Einstein-de Sitter universe is characterized by a cosmic fluid containing only matter. In this model, H_0 is the sole free parameter, i.e., $\theta = \{H_0\}$, and the Hubble rate is expressed as

$$H^{\text{EdS}}(z, \theta) = H_0(1+z)^{3/2}. \quad (5)$$

With the flat prior on $H_0 \in [0, 150] \text{ km s}^{-1} \text{Mpc}^{-1}$, we find that a low upper limit of $h_0 < 0.401$ is required in order to ensure the Universe is older than the OAO (see the right panel of Figure 4). The Einstein-de Sitter universe can thus be safely excluded, given that this inferred upper limit on H_0 is in 25.5σ tension with the locally measured H_0 .

3. A COSMOLOGY-INDEPENDENT ESTIMATE OF THE SPATIAL CURVATURE

In this section, we obtain the curvature-dependent luminosity distance to the OAO, based on their age measurements, and estimate the spatial curvature constant by comparing it with the empirically derived distance modulus of SNe Ia.

3.1. Curvature-dependent distance from the age of OAO

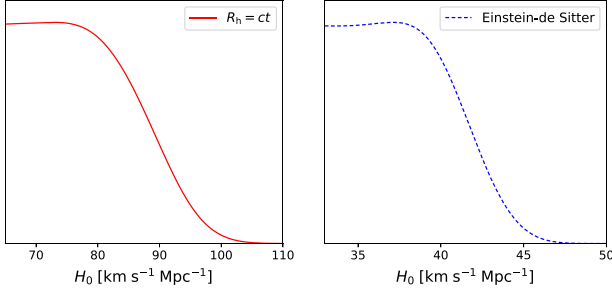


Figure 4. 1D posterior distributions of the Hubble constant H_0 in the $R_h = ct$ universe (left panel) and the Einstein-de Sitter universe (right panel), constrained by the 114 age-redshift data.

In the FLRW spacetime, the luminosity distance $D_L(z)$ may be written using the first derivative of the age, t , of the Universe,

$$D_L(z) = \frac{c}{H_0} \frac{(1+z)}{\sqrt{|\Omega_k|}} \times \text{sinn} \left\{ H_0 \sqrt{|\Omega_k|} \int_z^0 (1+z') \frac{dt}{dz'} dz' \right\}. \quad (6)$$

In this expression, sinn is sinh when $\Omega_k > 0$ and sin when $\Omega_k < 0$. For a flat universe with $\Omega_k = 0$, the right-hand side of this expression simplifies to the form $(1+z)c$ times the integral. Thus, if one can access the quantity dt/dz at the required redshift, without pre-assuming a particular cosmological model, one may reconstruct the line-of-sight comoving distance $D_C(z) = c \int_z^0 (1+z) \frac{dt}{dz'} dz'$ along with the curvature-dependent luminosity distance, $D_L(\Omega_k; z)$. The idea that dt/dz may be obtained from the age-redshift measurements of old objects has been suggested on various occasions (Jimenez & Loeb 2002; Jesus et al. 2017; Rana et al. 2017).

Since we are primarily interested in the derivative dt/dz and the present age of the Universe from other observations, and much less so in the incubation time τ_{inc} , we choose to directly fit the original estimated ages $t_{\text{obj}}(z)$ of the OAO. Taking τ_{inc} to be constant, one may see that $t(z)$ differs from $t_{\text{obj}}(z)$ by just a constant. That is,

$$t(z) = t_{\text{obj}}(z) + \tau_{\text{inc}}. \quad (7)$$

In principle, we may use the age-redshift data of all 114 OAO up to $z \sim 8$ compiled by Vagnozzi et al. (2021b) to estimate dt/dz . However, this catalog includes two different kinds of source, viz., 61 galaxies and 53 quasars, each of which has its own distinct incubation time. For this analysis, we therefore only employ the age of 61 galaxies distributed over the redshift interval $0.001 \leq z \leq 6.689$ to estimate dt/dz . The advantage of solely using galaxies is the relative uniformity

of the sample.² The originally estimated ages, t_{obj} , of the 61 galaxies are indicated as a function of redshift by the black points in Figure 1.

In our analysis, we construct the age function $t_{\text{obj}}(z)$ in a cosmology-independent way by fitting a third-order polynomial, with the initial condition $t_{\text{obj}}(z \rightarrow \infty) = 0$, to the age-redshift data. To mitigate the convergence problem that the polynomial fit encounters at high redshifts, we recast the $t_{\text{obj}}(z)$ function in the form of the y -redshift, defined by the relation $y = z/(1+z)$. In this way, the age in $z \in [0, \infty)$ is mapped into $y \in [0, 1]$, so that the polynomial fit is well behaved throughout the redshift range from our local Universe to the Big Bang. This polynomial is then expressed as

$$t_{\text{obj}}(y) = a_0 + a_1 y + a_2 y^2 + a_3 y^3, \quad (8)$$

where a_1 , a_2 , and a_3 are three free parameters (all in units of Gyr). With the initial condition $t_{\text{obj}}(z \rightarrow \infty) = t_{\text{obj}}(y = 1) = 0$, it is easy to identify $a_0 \equiv -a_1 - a_2 - a_3$. For $z = 0$, Equation (7) simplifies to $t_0 = a_0 + \tau_{\text{inc}}$. Once we have the inferred value of a_0 and know the present age of the Universe t_0 , we can also estimate τ_{inc} .

As we assume τ_{inc} to be constant, we have $\frac{dt_{\text{obj}}}{dz} = \frac{dt}{dz}$. Thus, by differentiating the polynomial (Eqn. 8), we obtain

$$\frac{dt}{dz} = \frac{a_1}{(1+z)^2} + \frac{2a_2 z}{(1+z)^3} + \frac{3a_3 z^2}{(1+z)^4}. \quad (9)$$

Then, the curvature-dependent luminosity distance can be derived by substituting Equation (9) into (6), i.e.,

$$D_L(z) = \frac{c}{H_0} \frac{(1+z)}{\sqrt{|\Omega_k|}} \text{sinn} \left\{ H_0 \sqrt{|\Omega_k|} \int_z^0 \left[\frac{a_1}{1+z'} + \frac{2a_2 z'}{(1+z')^2} + \frac{3a_3 z'^2}{(1+z')^3} \right] dz' \right\}. \quad (10)$$

We can further obtain the reconstructed distance modulus $\mu_{\text{age}}(\Omega_k, a_1, a_2, a_3; z)$ using the age-redshift data:

$$\mu_{\text{age}}(\Omega_k, a_1, a_2, a_3; z) = 5 \log_{10} \left[\frac{D_L(z)}{\text{Mpc}} \right] + 25. \quad (11)$$

3.2. Distance from observations of SNe Ia

By comparing the curvature-dependent luminosity distance $D_L(\Omega_k, z)$ derived from the age-redshift data with the empirically-derived luminosity distance (at similar redshifts) we can obtain a model-independent measurement of Ω_k . For the latter, we use the largest Pantheon SN Ia sample, consisting of 1,048 SNe Ia in the redshift range $0.01 < z < 2.3$ (Scolnic et al. 2018).

² Note, however, that there is no guarantee that all the galaxies constitute a homogeneous sample either. This analysis should perhaps be carried out for each sub-sample separately. But since the current sub-sample size is admittedly small, we use all the galaxies for our analysis.

The observed distance modulus of each SN is given as

$$\mu_{\text{SN}} = m_B + \alpha x_1 - \beta \mathcal{C} - M_B^*, \quad (12)$$

where m_B is the observed B -band apparent magnitude, x_1 is the light-curve stretch factor, and \mathcal{C} is the SN color at maximum brightness. The absolute B -band magnitude M_B^* is correlated with the host galaxy mass M_{stellar} via a simple step function (Betoule et al. 2014; Scolnic et al. 2018):

$$M_B^* = \begin{cases} M_B + \Delta_M & \text{for } M_{\text{stellar}} > 10^{10} M_{\odot} \\ M_B & \text{otherwise,} \end{cases} \quad (13)$$

where Δ_M corresponds to a distance correction based on M_{stellar} . Note that α , β , M_B , and Δ_M are nuisance parameters that need to be constrained simultaneously with the cosmological parameters. As such, the derived SN distance is typically dependent on the chosen cosmology. To avoid this, Kessler & Scolnic (2017) introduced an approximate method called BEAMS with Bias Corrections (BBC) to correct those expected biases and simultaneously fit for the SN nuisance parameters. The BBC fit produces a bin-averaged Hubble diagram of SNe Ia, and then the nuisance parameters α and β are constrained by fitting to a reference cosmological model with fixed values of the matter density Ω_m and equation-of-state of dark energy w . Within each redshift bin, the local shape of the Hubble diagram is assumed to be well described by the reference cosmological model. If there are sufficient redshift bins, the fitted parameters α and β will converge to consistent values (Marriner et al. 2011; Kessler & Scolnic 2017).

With the BBC method, Scolnic et al. (2018) report the corrected apparent magnitudes $m_{\text{corr}} = m_B + \alpha x_1 - \beta \mathcal{C} - \Delta_M + \Delta_B$ for all the SNe, where Δ_B is the added distance correction. Given these corrected apparent magnitudes, we just need to subtract the absolute magnitude M_B from m_{corr} to derive the observed distance moduli:

$$\mu_{\text{SN}} = m_{\text{corr}} - M_B. \quad (14)$$

The caveat with this approach, however, is that the format assumes all cosmological models are nested, which is not true in general. This formulation may be used approximately for various versions of Λ CDM, but not for other models, such as $R_h = ct$, whose luminosity distance does not depend on parameters such as Ω_k . The caveat here is that the results we report below pertain specifically to Λ CDM, not necessarily to other FLRW models, or models based on alternative theories of gravity.

Even within the context of Λ CDM, however, there may still be some residual model dependence, so to test how serious this limitation might be, we take the following approach. The inferred values of α and β in the BBC method are valid

only for the reference model. We therefore consider two different cases: first, the determination of α and β is assumed to be independent of the model, and we directly use those corrected apparent magnitudes reported by Scolnic et al. (2018) for our purpose; second, we carry out a parallel analysis of the uncorrected SN magnitudes by re-constraining α and β as nuisance parameters, and we compare the results.

3.3. Analysis and results

We constrain all of the free parameters via a joint analysis involving the galaxy age and SN Ia data. The final log-likelihood sampled by the Python MCMC module EMCEE is a sum of the separate likelihoods of the galaxy ages and SNe Ia:

$$\ln(\mathcal{L}_{\text{tot}}) = \ln(\mathcal{L}_{t_{\text{obj}}}) + \ln(\mathcal{L}_{\text{SN}}), \quad (15)$$

where

$$\ln(\mathcal{L}_{t_{\text{obj}}}) = -\frac{1}{2} \sum_i^{61} \frac{[t_{\text{obj},i}^{\text{obs}} - t_{\text{obj},i}^{\text{fit}}(a_1, a_2, a_3; z_i)]^2}{\sigma_{t_{\text{obj},i}}^2} \quad (16)$$

and

$$-2 \ln(\mathcal{L}_{\text{SN}}) = \Delta \hat{\mu}^T \cdot \mathbf{Cov}^{-1} \cdot \Delta \hat{\mu}. \quad (17)$$

In Equation (16), $\sigma_{t_{\text{obj},i}}$ is the uncertainty of the i -th age measurement $t_{\text{obj},i}^{\text{obs}}$ and $t_{\text{obj},i}^{\text{fit}}(a_1, a_2, a_3; z_i)$ is obtained from Equation (8). In Equation (17), $\Delta \hat{\mu} = \hat{\mu}_{\text{SN}}(M_B; z) - \hat{\mu}_{\text{age}}(\Omega_k, a_1, a_2, a_3; z)$ is the data vector, defined by the difference between the distance modulus μ_{SN} of SNe Ia (Eqn. 14) and the constructed distance modulus μ_{age} from the galaxy age-redshift data (Eqn. 11), and \mathbf{Cov} is a full covariance matrix that contains both statistical and systematic uncertainties of SNe. Note that in the SN likelihood estimation, there is a degeneracy between H_0 and M_B . We therefore adopt a fiducial $H_0 = 70 \text{ km s}^{-1} \text{ Mpc}^{-1}$ for the sake of constraining M_B . In this case, the free parameters are: the spatial curvature parameter Ω_k , the three polynomial coefficients (a_1, a_2, a_3) , and the SN absolute magnitude M_B .

The 1D marginalized posterior distributions and 2D regions with $1 - 2\sigma$ contours corresponding to these five free parameters, constrained by the galaxy ages and corrected SN magnitudes, are presented in Figure 5. These contours show that, at the 1σ confidence level, the inferred parameter values are $\Omega_k = 0.43_{-0.27}^{+0.27}$, $a_1 = -14.21_{-1.46}^{+1.44}$, $a_2 = -5.37_{-0.95}^{+0.91}$, $a_3 = 6.76_{-1.13}^{+1.15}$, and $M_B = -19.40_{-0.21}^{+0.23}$. The corresponding results for the galaxy + corrected SN data are summarized in Table 2. With this approach, we find that the spatial geometry of the Universe is marginally consistent with spatial flatness at a 1.6σ level of confidence.

As noted earlier, our procedure allows us to determine the inferred value of a_0 along with the best-fit polynomial coefficients, i.e., $a_0 \equiv -a_1 - a_2 - a_3 = 12.82 \pm 2.06 \text{ Gyr}$. Considering the present age of the Universe as inferred from

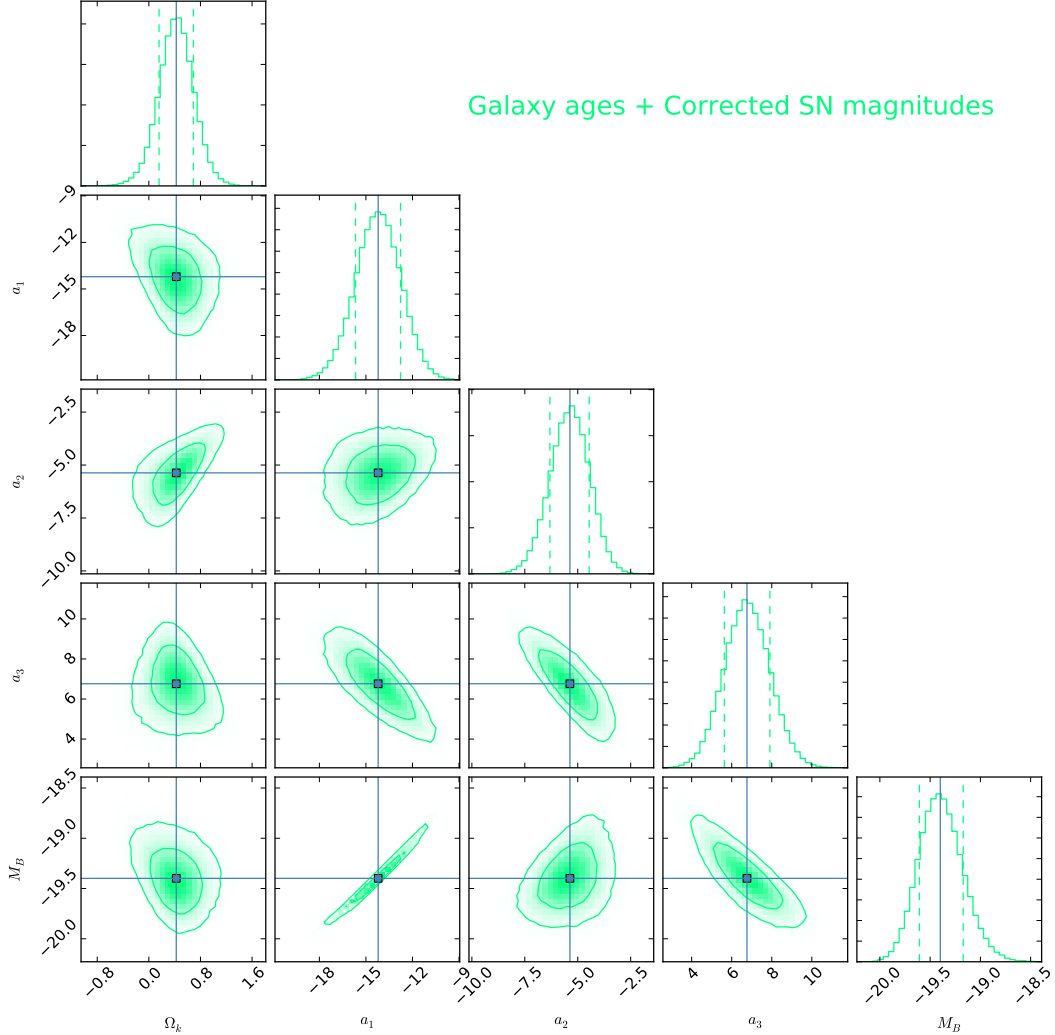


Figure 5. 1D and 2D marginalized posterior distributions with the 1–2 σ contours for the cosmic curvature Ω_k , the polynomial coefficients (a_1 , a_2 , a_3), and the SN absolute magnitude M_B , based on the joint analysis of the galaxy age and corrected SN magnitude data. The vertical solid lines represent the medium parameter values, whereas the vertical dashed lines indicate $\pm 1\sigma$ deviations from their respective means.

Table 2. Constraints on all parameters with different choices of data

Data	Ω_k	a_1 (Gyr)	a_2 (Gyr)	a_3 (Gyr)	M_B	α	β	Δ_M	σ_{int}
galaxy + corrected SN	$0.43^{+0.27}_{-0.27}$	$-14.21^{+1.44}_{-1.46}$	$-5.37^{+0.91}_{-0.95}$	$6.76^{+1.15}_{-1.13}$	$-19.40^{+0.23}_{-0.21}$	–	–	–	–
galaxy + uncorrected SN	$0.59^{+0.18}_{-0.17}$	$-15.28^{+1.53}_{-1.54}$	$-3.78^{+0.71}_{-0.74}$	$6.02^{+1.06}_{-1.05}$	$-19.48^{+0.23}_{-0.21}$	$0.132^{+0.005}_{-0.005}$	$2.595^{+0.057}_{-0.056}$	$0.052^{+0.009}_{-0.009}$	$0.079^{+0.006}_{-0.006}$

Planck in the context flat Λ CDM ($t_0 = 13.80 \pm 0.02$ Gyr; [Planck Collaboration et al. 2020](#)), we can further estimate the incubation time as $\tau_{\text{inc}} = t_0 - a_0 = 0.98 \pm 2.06$ Gyr.

Next, to investigate how sensitive our results of Ω_k are to the choice of corrected SN magnitudes provided by the Pantheon team, we also perform a (parallel) comparative analysis of the galaxy + uncorrected SN data by simultaneously constraining the nuisance parameters along with Ω_k . The likeli-

hood function of SNe now becomes

$$\mathcal{L}_{\text{SN}} = \prod_{i=1}^{1048} \frac{1}{\sqrt{2\pi}\sigma_{\text{stat},i}} \exp\left(-\frac{\Delta\mu_i^2}{2\sigma_{\text{stat},i}^2}\right), \quad (18)$$

where $\Delta\mu_i = \mu_{\text{SN}}(\alpha, \beta, M_B, \Delta_M; z_i) - \mu_{\text{age}}(\Omega_k, a_1, a_2, a_3; z_i)$ is the difference between the distance modulus μ_{SN} of SN Ia (Eqn. 12) and the distance modulus μ_{age} constructed from the galaxy age-redshift data (Eqn. 11), and $\sigma_{\text{stat},i}$ is the statistical

uncertainty of each SN, given by the expression

$$\begin{aligned} \sigma_{\text{stat},i}^2 = & \sigma_{m_B,i}^2 + \alpha^2 \sigma_{x_1,i}^2 + \beta^2 \sigma_{\mathcal{C},i}^2 \\ & + 2\alpha C_{m_B x_1,i} - 2\beta C_{m_B \mathcal{C},i} - 2\alpha\beta C_{x_1 \mathcal{C},i} \\ & + \sigma_{\mu-z,i}^2 + \sigma_{\text{lens},i}^2 + \sigma_{\text{int}}^2. \end{aligned} \quad (19)$$

Here, $\sigma_{m_B,i}$, $\sigma_{x_1,i}$, and $\sigma_{\mathcal{C},i}$ stand for the uncertainties of the peak magnitude and light-curve parameters of the i -th SN, the terms $C_{m_B x_1,i}$, $C_{m_B \mathcal{C},i}$, and $C_{x_1 \mathcal{C},i}$ represent the covariances among m_B , x_1 , \mathcal{C} for the i -th SN, $\sigma_{\text{lens},i}$ is the uncertainty from stochastic gravitational lensing, and σ_{int} is the unknown intrinsic uncertainty. The dispersion $\sigma_{\mu-z,i} = 5\sqrt{\sigma_{z_{\text{pec}}}^2 + \sigma_{z_i}^2} / (z_i \ln 10)$ accounts for the uncertainty from the peculiar velocity uncertainty $\sigma_{z_{\text{pec}}}$ and redshift measurement uncertainty σ_{z_i} in quadrature. We follow [Scolnic et al. \(2018\)](#) in using $c\sigma_{z_{\text{pec}}} = 240 \text{ km s}^{-1}$, as well as $\sigma_{\text{lens},i} = 0.055z_i$.

Only the statistical uncertainties are considered since the six-parameter systematic covariance matrices (m_B , x_1 , \mathcal{C} , $m_B \mathcal{C}$, $x_1 m_B$, $x_1 \mathcal{C}$) are not available in [Scolnic et al. \(2018\)](#). In this case, the free parameters are the curvature parameter Ω_k , the three polynomial coefficients (a_1 , a_2 , a_3), and the SN nuisance parameters (α , β , M_B , Δ_M , σ_{int}). These nine parameters are constrained to be $\Omega_k = 0.59_{-0.17}^{+0.18}$, $a_1 = -15.28_{-1.54}^{+1.53}$, $a_2 = -3.78_{-0.74}^{+0.71}$, $a_3 = 6.02_{-1.05}^{+1.06}$, $\alpha = 0.132_{-0.005}^{+0.005}$, $\beta = 2.595_{-0.056}^{+0.057}$, $M_B = -19.48_{-0.21}^{+0.23}$, $\Delta_M = 0.052_{-0.009}^{+0.009}$, and $\sigma_{\text{int}} = 0.079_{-0.006}^{+0.006}$, which are displayed in Figure 6 and summarized in Table 2. The comparison between lines 1 and 2 of Table 2 suggests that simply using the corrected SN magnitudes introduces a non-negligible disparity in the results. The value of Ω_k inferred from the galaxy + corrected SN data represents a 0.5σ tension with that measured from the galaxy + uncorrected SN data.

4. SUMMARY AND DISCUSSION

In this work, we have used the age measurements of 114 OAO (including 61 galaxies and 53 quasars) in the redshift range $0 \lesssim z \lesssim 8$ to constrain the late-time cosmic expansion history and explore the Hubble tension in several cosmological models. Owing to the age of the Universe at any redshift being inversely proportional to the Hubble constant H_0 , the requirement that the Universe be older than the OAO it contains at any redshift provides an upper limit to H_0 .

Assuming the validity of flat Λ CDM at late times, and setting wide flat priors on H_0 and Ω_m , we have obtained $H_0 < 75.5 \text{ km s}^{-1} \text{ Mpc}^{-1}$ at the 95% confidence level, roughly consistent with local H_0 measurements. However, if a Gaussian prior of $\Omega_m = 0.315 \pm 0.007$ informed by *Planck* is used, then the 95% confidence level upper limit on H_0 turned out to be $H_0 < 70.6 \text{ km s}^{-1} \text{ Mpc}^{-1}$, representing a 2σ tension with the locally measured value. It is compatible with the *Planck* inference, however. This is interesting because, in this scenario, both H_0 and Ω_m are mutually consistent for

both *Planck* and the OAO age-redshift data. We found that the inferred upper value to H_0 does depend quite significantly on Ω_m . Since the local measurement of H_0 does not require Ω_m , while *Planck* uses both, we conclude that the Hubble tension between the two measurements may be due in part to the use of Ω_m in one case and not the other.

Besides Λ CDM, we also discussed how the H_0 limits may be obtained for $R_h = ct$ and Einstein-de Sitter. The $R_h = ct$ universe fits the age-redshift data with an upper limit of $H_0 < 86.1 \text{ km s}^{-1} \text{ Mpc}^{-1}$. By comparison, the Einstein-de Sitter universe fits the same data with an upper limit of $H_0 < 40.1 \text{ km s}^{-1} \text{ Mpc}^{-1}$. Obviously, Einstein-de Sitter fails to pass the cosmic age test, because the inferred upper limit to H_0 in this model represents a 25.5σ tension with the locally measured H_0 . Our overall results affirm the idea that cosmic ages are an extremely valuable probe in the quest towards uncovering the nature of the Hubble tension.

We have also proposed a novel method of estimating the spatial curvature, avoiding possible biases introduced by the pre-assumption of a specific cosmological model. To perform our analysis, we have considered the following cosmological data: 61 age measurements of galaxies and 1,048 SNe Ia from Pantheon compilation. Based on the geometric relation in the FLRW metric, we have shown the possibility of obtaining the curvature-dependent luminosity distance from a best-fit polynomial to the age-redshift data of old objects. By comparing this curvature-dependent luminosity distance with the empirical luminosity distance inferred from SNe Ia, we obtained a somewhat model-independent estimate of the curvature parameter Ω_k based on the parametrization in Λ CDM.

[Scolnic et al. \(2018\)](#) applied the BBC method to determine the SN nuisance parameters and reported the corrected apparent magnitudes for all the Pantheon SNe. Combining the age-redshift measurements of galaxies with these corrected SN magnitudes, we have placed limits simultaneously on the cosmic curvature Ω_k , the polynomial coefficients (a_1 , a_2 , a_3), and the SN absolute magnitude M_B . This analysis suggests that the curvature parameter is constrained to be $\Omega_k = 0.43_{-0.27}^{+0.27}$, which marginally compatible with zero. That is, the spatial geometry of the Universe is marginally consistent with spatial flatness at the 1.6σ level.

As the inferred values of the SN nuisance parameters in the BBC method may depend on the reference cosmological model, even within the context of Λ CDM, we also carried out this type of analysis using the combined galaxy + uncorrected SN data sets by simultaneously constraining the curvature parameter Ω_k , the polynomial coefficients (a_1 , a_2 , a_3), and the SN nuisance parameters (α , β , M_B , Δ_M , σ_{int}). In this case, we found that the constraint is $\Omega_k = 0.59_{-0.17}^{+0.18}$. The value of Ω_k changes slightly, by about 0.5σ , when the SN nuisance parameters are re-constrained along with the cosmology, im-

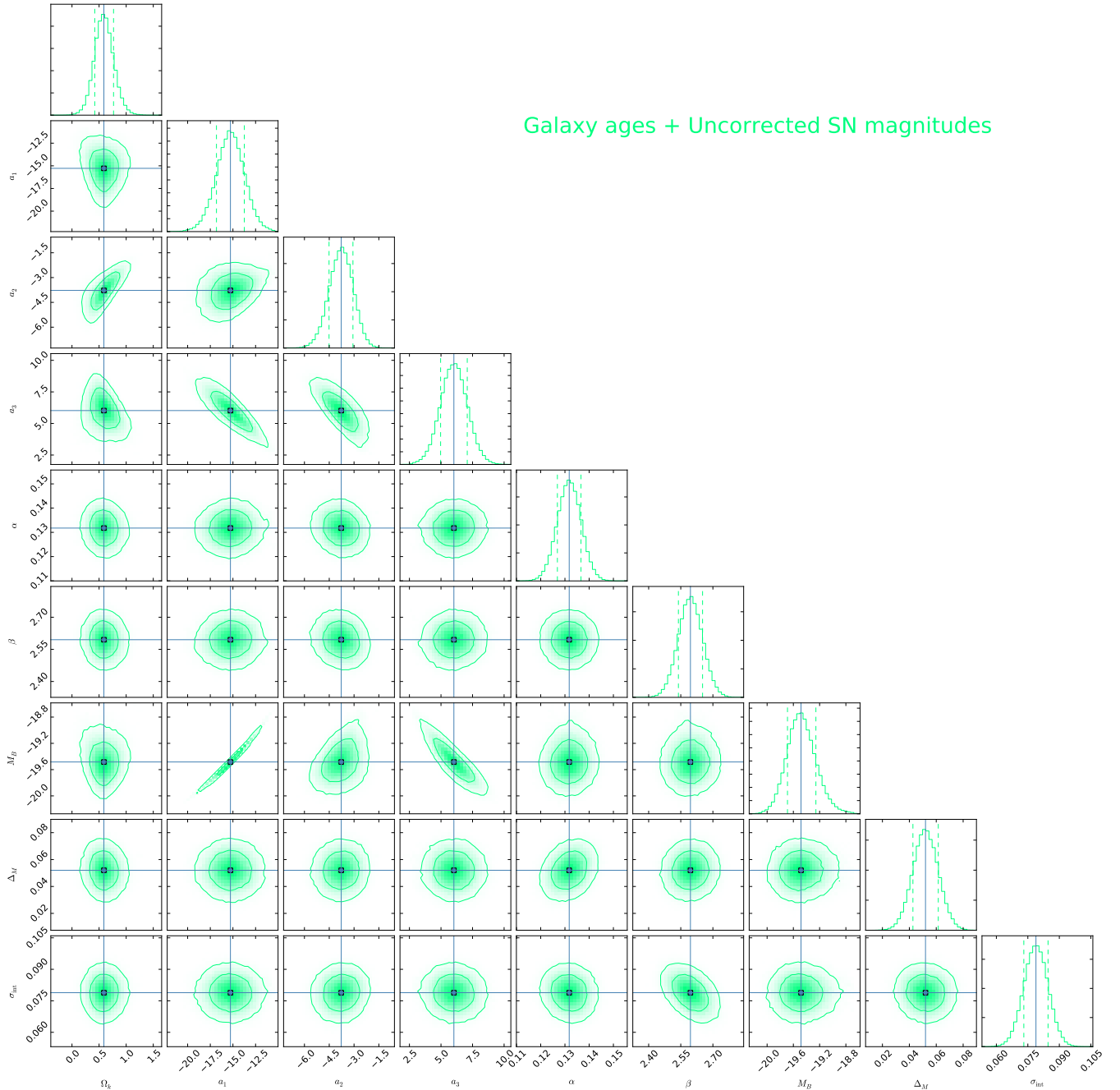


Figure 6. Same as Figure 5, but now showing the constraints for the parameters Ω_k , a_1 , a_2 , a_3 , α , β , M_B , Δ_M , and σ_{int} based on the joint analysis of the galaxy age and uncorrected SN magnitude data.

plying that simply using the corrected SN magnitudes would introduce a non-negligible disparity in the results.

Such deviations from zero are not yet compelling enough to initiate a detailed investigation of their implications. We point out, however, that there are several rather essential consequences, should such an outcome be realized. First, spatial flatness is assumed to be an indicator of inflation (Guth 1981). If the Universe is not spatially flat after all, this would cast serious doubt on the possibility that inflation could have happened. At the very least, it would require major modifi-

cations to most of the inflation potentials proposed thus far. Note, however, that a de Sitter expansion need not necessarily proceed solely with spatial flatness. As such, several attempts have been made to create an inflationary scenario with negative spatial curvature, leading to an open Universe. This may happen, e.g., in the context of quantum tunnelling-induced false vacuum decay (Ratra 1994; Ratra & Peebles 1994, 1995; Bucher et al. 1995; Kleban & Schillo 2012).

Second, if it turns out that Ω_k is definitely positive, the Universe must also have net positive energy density (Melia

2020). This would be very alarming in the context of a quantum-fluctuation origin for the Big Bang, since it would rule out a ‘creation from nothing’ scenario, in which all the laws of physics, initial conditions and all the structure appeared as a quantum fluctuation at $t = 0$ with no pre-history. It would at the very least imply a pre-existing vacuum prior to the expansionary event. Even so, one would then need to contend with the very serious problem of how a Universe with the known value of Planck’s constant and such an enormous amount of energy could have lived long enough to classicalize and evolve into the large-scale structure we see today (Melia 2020).

There are good philosophical, if not empirical, reasons for believing that Ω_k must be zero. But we cannot yet make that claim without at least some doubt, certainly not based on the

analysis of the oldest astronomical objects in the Universe that we have carried out in this paper.

1 We are grateful to Sunny Vagnozzi for systematically assembling the high- z OAO catalog and sharing it with us. JJW
2 would like to thank Yan-Mei Han for her infinite patience
3 while part of this project was carried out at home during
4 the Nanjing lockdown caused by the Covid-19 pandemic.
5 This work is partially supported by the National Natural Science
6 Foundation of China (grant Nos. 11725314, U1831122,
7 and 12041306), the Youth Innovation Promotion Association
8 (2017366), the Key Research Program of Frontier Sciences
9 (grant No. ZDBS-LY-7014) of Chinese Academy of Sciences,
10 the Major Science and Technology Project of Qinghai
11 Province (2019-ZJ-A10), the China Manned Space Project
12 (CMS-CSST-2021-B11), and the Guangxi Key Laboratory
13 for Relativistic Astrophysics. We are also grateful to the
14 anonymous referee for helpful comments.
15

REFERENCES

- Alcaniz, J. S., & Lima, J. A. S. 1999, *ApJL*, 521, L87, doi: [10.1086/312191](https://doi.org/10.1086/312191)
- Aubourg, É., Bailey, S., Bautista, J. E., et al. 2015, *PhRvD*, 92, 123516, doi: [10.1103/PhysRevD.92.123516](https://doi.org/10.1103/PhysRevD.92.123516)
- Bañados, E., Venemans, B. P., Mazzucchelli, C., et al. 2018, *Nature*, 553, 473, doi: [10.1038/nature25180](https://doi.org/10.1038/nature25180)
- Bengaly, C. A. P., Dantas, M. A., Carvalho, J. C., & Alcaniz, J. S. 2014, *A&A*, 561, A44, doi: [10.1051/0004-6361/201322475](https://doi.org/10.1051/0004-6361/201322475)
- Bernal, J. L., Verde, L., Jimenez, R., et al. 2021, *PhRvD*, 103, 103533, doi: [10.1103/PhysRevD.103.103533](https://doi.org/10.1103/PhysRevD.103.103533)
- Bernstein, G. 2006, *ApJ*, 637, 598, doi: [10.1086/498079](https://doi.org/10.1086/498079)
- Betoule, M., Kessler, R., Guy, J., et al. 2014, *A&A*, 568, A22, doi: [10.1051/0004-6361/201423413](https://doi.org/10.1051/0004-6361/201423413)
- Bolte, M., & Hogan, C. J. 1995, *Nature*, 376, 399, doi: [10.1038/376399a0](https://doi.org/10.1038/376399a0)
- Boylan-Kolchin, M., & Weisz, D. R. 2021, *MNRAS*, 505, 2764, doi: [10.1093/mnras/stab1521](https://doi.org/10.1093/mnras/stab1521)
- Bucher, M., Goldhaber, A. S., & Turok, N. 1995, *PhRvD*, 52, 3314, doi: [10.1103/PhysRevD.52.3314](https://doi.org/10.1103/PhysRevD.52.3314)
- Cai, R.-G., Guo, Z.-K., & Yang, T. 2016, *PhRvD*, 93, 043517, doi: [10.1103/PhysRevD.93.043517](https://doi.org/10.1103/PhysRevD.93.043517)
- Cao, S., Liu, T., Biesiada, M., et al. 2021, arXiv e-prints, arXiv:2112.00237. <https://arxiv.org/abs/2112.00237>
- Cao, S., Qi, J., Biesiada, M., et al. 2019a, *Physics of the Dark Universe*, 24, 100274, doi: [10.1016/j.dark.2019.100274](https://doi.org/10.1016/j.dark.2019.100274)
- Cao, S., Qi, J., Cao, Z., et al. 2019b, *Scientific Reports*, 9, 11608, doi: [10.1038/s41598-019-47616-4](https://doi.org/10.1038/s41598-019-47616-4)
- Capozziello, S., Cardone, V. F., Funaro, M., & Andreon, S. 2004, *PhRvD*, 70, 123501, doi: [10.1103/PhysRevD.70.123501](https://doi.org/10.1103/PhysRevD.70.123501)
- Clarkson, C., Cortês, M., & Bassett, B. 2007, *JCAP*, 2007, 011, doi: [10.1088/1475-7516/2007/08/011](https://doi.org/10.1088/1475-7516/2007/08/011)
- Collett, T., Montanari, F., & Räsänen, S. 2019, *PhRvL*, 123, 231101, doi: [10.1103/PhysRevLett.123.231101](https://doi.org/10.1103/PhysRevLett.123.231101)
- Dainotti, M. G., De Simone, B., Schiavone, T., et al. 2021, *ApJ*, 912, 150, doi: [10.3847/1538-4357/abeb73](https://doi.org/10.3847/1538-4357/abeb73)
- Dantas, M. A., Alcaniz, J. S., Jain, D., & Dev, A. 2007, *A&A*, 467, 421, doi: [10.1051/0004-6361:20066632](https://doi.org/10.1051/0004-6361:20066632)
- Dantas, M. A., Alcaniz, J. S., Mania, D., & Ratra, B. 2011, *Physics Letters B*, 699, 239, doi: [10.1016/j.physletb.2011.04.014](https://doi.org/10.1016/j.physletb.2011.04.014)
- Dantas, M. A., Alcaniz, J. S., & Pires, N. 2009, *Physics Letters B*, 679, 423, doi: [10.1016/j.physletb.2009.08.008](https://doi.org/10.1016/j.physletb.2009.08.008)
- Denissenya, M., Linder, E. V., & Shafieloo, A. 2018, *JCAP*, 2018, 041, doi: [10.1088/1475-7516/2018/03/041](https://doi.org/10.1088/1475-7516/2018/03/041)
- Dhawan, S., Alsing, J., & Vagnozzi, S. 2021, *MNRAS*, 506, L1, doi: [10.1093/mnras/lsab058](https://doi.org/10.1093/mnras/lsab058)
- Di Valentino, E., Mena, O., Pan, S., et al. 2021, *Classical and Quantum Gravity*, 38, 153001, doi: [10.1088/1361-6382/ac086d](https://doi.org/10.1088/1361-6382/ac086d)
- Dunlop, J., Peacock, J., Spinrad, H., et al. 1996, *Nature*, 381, 581, doi: [10.1038/381581a0](https://doi.org/10.1038/381581a0)
- Eisenstein, D. J., Zehavi, I., Hogg, D. W., et al. 2005, *ApJ*, 633, 560, doi: [10.1086/466512](https://doi.org/10.1086/466512)
- Foreman-Mackey, D., Hogg, D. W., Lang, D., & Goodman, J. 2013, *PASP*, 125, 306, doi: [10.1086/670067](https://doi.org/10.1086/670067)
- Friça, A. C. S., Alcaniz, J. S., & Lima, J. A. S. 2005, *MNRAS*, 362, 1295, doi: [10.1111/j.1365-2966.2005.09401.x](https://doi.org/10.1111/j.1365-2966.2005.09401.x)
- Gong, Y., & Wang, A. 2007, *PhRvD*, 75, 043520, doi: [10.1103/PhysRevD.75.043520](https://doi.org/10.1103/PhysRevD.75.043520)

- Grogin, N. A., Kocevski, D. D., Faber, S. M., et al. 2011, *ApJS*, 197, 35, doi: [10.1088/0067-0049/197/2/35](https://doi.org/10.1088/0067-0049/197/2/35)
- Guth, A. H. 1981, *PhRvD*, 23, 347, doi: [10.1103/PhysRevD.23.347](https://doi.org/10.1103/PhysRevD.23.347)
- Hubble, E. 1929, *Proceedings of the National Academy of Science*, 15, 168, doi: [10.1073/pnas.15.3.168](https://doi.org/10.1073/pnas.15.3.168)
- Ichikawa, K., Kawasaki, M., Sekiguchi, T., & Takahashi, T. 2006, *JCAP*, 2006, 005, doi: [10.1088/1475-7516/2006/12/005](https://doi.org/10.1088/1475-7516/2006/12/005)
- Jain, D., & Dev, A. 2006, *Physics Letters B*, 633, 436, doi: [10.1016/j.physletb.2005.12.007](https://doi.org/10.1016/j.physletb.2005.12.007)
- Jedamzik, K., Pogosian, L., & Zhao, G.-B. 2021, *Communications Physics*, 4, 123, doi: [10.1038/s42005-021-00628-x](https://doi.org/10.1038/s42005-021-00628-x)
- Jesus, J. F., Holanda, R. F. L., & Dantas, M. A. 2017, *General Relativity and Gravitation*, 49, 150, doi: [10.1007/s10714-017-2317-5](https://doi.org/10.1007/s10714-017-2317-5)
- Jesus, J. F., Valentim, R., Moraes, P. H. R. S., & Malheiro, M. 2021, *MNRAS*, 500, 2227, doi: [10.1093/mnras/staa3426](https://doi.org/10.1093/mnras/staa3426)
- Jimenez, R., Cimatti, A., Verde, L., Moresco, M., & Wandelt, B. 2019, *JCAP*, 2019, 043, doi: [10.1088/1475-7516/2019/03/043](https://doi.org/10.1088/1475-7516/2019/03/043)
- Jimenez, R., & Loeb, A. 2002, *ApJ*, 573, 37, doi: [10.1086/340549](https://doi.org/10.1086/340549)
- Jimenez, R., Verde, L., Treu, T., & Stern, D. 2003, *ApJ*, 593, 622, doi: [10.1086/376595](https://doi.org/10.1086/376595)
- Kessler, R., & Scolnic, D. 2017, *ApJ*, 836, 56, doi: [10.3847/1538-4357/836/1/56](https://doi.org/10.3847/1538-4357/836/1/56)
- Kleban, M., & Schillo, M. 2012, *JCAP*, 2012, 029, doi: [10.1088/1475-7516/2012/06/029](https://doi.org/10.1088/1475-7516/2012/06/029)
- Krauss, L. M., & Turner, M. S. 1995, *General Relativity and Gravitation*, 27, 1137, doi: [10.1007/BF02108229](https://doi.org/10.1007/BF02108229)
- Krishnan, C., Colgáin, E. Ó., Ruchika, Sen, A. A., Sheikh-Jabbari, M. M., & Yang, T. 2020, *PhRvD*, 102, 103525, doi: [10.1103/PhysRevD.102.103525](https://doi.org/10.1103/PhysRevD.102.103525)
- Krishnan, C., Mohayaee, R., Colgáin, E. Ó., Sheikh-Jabbari, M. M., & Yin, L. 2021a, *Classical and Quantum Gravity*, 38, 184001, doi: [10.1088/1361-6382/ac1a81](https://doi.org/10.1088/1361-6382/ac1a81)
- . 2021b, *arXiv e-prints*, arXiv:2106.02532, <https://arxiv.org/abs/2106.02532>
- Lemaître, G. 1927, *Annales de la Société Scientifique de Bruxelles*, 47, 49
- L'Huillier, B., & Shafieloo, A. 2017, *JCAP*, 2017, 015, doi: [10.1088/1475-7516/2017/01/015](https://doi.org/10.1088/1475-7516/2017/01/015)
- Li, E.-K., Du, M., & Xu, L. 2020, *MNRAS*, 491, 4960, doi: [10.1093/mnras/stz3308](https://doi.org/10.1093/mnras/stz3308)
- Li, S.-Y., Li, Y.-L., Zhang, T.-J., & Zhang, T. 2019a, *ApJ*, 887, 36, doi: [10.3847/1538-4357/ab5225](https://doi.org/10.3847/1538-4357/ab5225)
- Li, Y., Fan, X., & Gou, L. 2019b, *ApJ*, 873, 37, doi: [10.3847/1538-4357/ab037e](https://doi.org/10.3847/1538-4357/ab037e)
- Li, Y.-L., Li, S.-Y., Zhang, T.-J., & Li, T.-P. 2014, *ApJL*, 789, L15, doi: [10.1088/2041-8205/789/1/L15](https://doi.org/10.1088/2041-8205/789/1/L15)
- Li, Z., Ding, X., Wang, G.-J., Liao, K., & Zhu, Z.-H. 2018a, *ApJ*, 854, 146, doi: [10.3847/1538-4357/aaa76f](https://doi.org/10.3847/1538-4357/aaa76f)
- Li, Z., Wang, G.-J., Liao, K., & Zhu, Z.-H. 2016, *ApJ*, 833, 240, doi: [10.3847/1538-4357/833/2/240](https://doi.org/10.3847/1538-4357/833/2/240)
- Li, Z.-X., Gao, H., Ding, X.-H., Wang, G.-J., & Zhang, B. 2018b, *Nature Communications*, 9, 3833, doi: [10.1038/s41467-018-06303-0](https://doi.org/10.1038/s41467-018-06303-0)
- Liao, K. 2019, *PhRvD*, 99, 083514, doi: [10.1103/PhysRevD.99.083514](https://doi.org/10.1103/PhysRevD.99.083514)
- Liao, K., Li, Z., Wang, G.-J., & Fan, X.-L. 2017, *ApJ*, 839, 70, doi: [10.3847/1538-4357/aa697e](https://doi.org/10.3847/1538-4357/aa697e)
- Lima, J. A. S., & Alcaniz, J. S. 2000, *MNRAS*, 317, 893, doi: [10.1046/j.1365-8711.2000.03695.x](https://doi.org/10.1046/j.1365-8711.2000.03695.x)
- Lin, W., Chen, X., & Mack, K. J. 2021, *ApJ*, 920, 159, doi: [10.3847/1538-4357/ac12cf](https://doi.org/10.3847/1538-4357/ac12cf)
- Liu, T., Cao, S., Zhang, J., et al. 2020, *MNRAS*, 496, 708, doi: [10.1093/mnras/staa1539](https://doi.org/10.1093/mnras/staa1539)
- Marriner, J., Bernstein, J. P., Kessler, R., et al. 2011, *ApJ*, 740, 72, doi: [10.1088/0004-637X/740/2/72](https://doi.org/10.1088/0004-637X/740/2/72)
- Matsuoka, Y., Onoue, M., Kashikawa, N., et al. 2019a, *ApJL*, 872, L2, doi: [10.3847/2041-8213/ab0216](https://doi.org/10.3847/2041-8213/ab0216)
- Matsuoka, Y., Iwasawa, K., Onoue, M., et al. 2019b, *ApJ*, 883, 183, doi: [10.3847/1538-4357/ab3c60](https://doi.org/10.3847/1538-4357/ab3c60)
- Mazzucchelli, C., Bañados, E., Venemans, B. P., et al. 2017, *ApJ*, 849, 91, doi: [10.3847/1538-4357/aa9185](https://doi.org/10.3847/1538-4357/aa9185)
- Melia, F. 2003, *The Edge of Infinity: Supermassive Black Holes in the Universe* (Cambridge University Press), doi: [10.1017/CBO9780511536366](https://doi.org/10.1017/CBO9780511536366)
- Melia, F. 2007, *MNRAS*, 382, 1917, doi: [10.1111/j.1365-2966.2007.12499.x](https://doi.org/10.1111/j.1365-2966.2007.12499.x)
- . 2013, *A&A*, 553, A76, doi: [10.1051/0004-6361/201220447](https://doi.org/10.1051/0004-6361/201220447)
- . 2020, *The Cosmic Spacetime* (Oxford: Taylor & Francis), doi: <https://doi.org/10.1201/9781003081029>
- Melia, F., & Shevchuk, A. S. H. 2012, *MNRAS*, 419, 2579, doi: [10.1111/j.1365-2966.2011.19906.x](https://doi.org/10.1111/j.1365-2966.2011.19906.x)
- Mortlock, D. J., Warren, S. J., Venemans, B. P., et al. 2011, *Nature*, 474, 616, doi: [10.1038/nature10159](https://doi.org/10.1038/nature10159)
- Nunes, R. C., & Pacucci, F. 2020, *MNRAS*, 496, 888, doi: [10.1093/mnras/staa1568](https://doi.org/10.1093/mnras/staa1568)
- Pacucci, F., Natarajan, P., Volonteri, M., Cappelluti, N., & Urry, C. M. 2017, *ApJL*, 850, L42, doi: [10.3847/2041-8213/aa9aea](https://doi.org/10.3847/2041-8213/aa9aea)
- Park, C.-G., & Ratra, B. 2019a, *Ap&SS*, 364, 82, doi: [10.1007/s10509-019-3567-3](https://doi.org/10.1007/s10509-019-3567-3)
- . 2019b, *ApJ*, 882, 158, doi: [10.3847/1538-4357/ab3641](https://doi.org/10.3847/1538-4357/ab3641)
- Pires, N., Zhu, Z.-H., & Alcaniz, J. S. 2006, *PhRvD*, 73, 123530, doi: [10.1103/PhysRevD.73.123530](https://doi.org/10.1103/PhysRevD.73.123530)
- Planck Collaboration, Aghanim, N., Akrami, Y., et al. 2020, *A&A*, 641, A6, doi: [10.1051/0004-6361/201833910](https://doi.org/10.1051/0004-6361/201833910)
- Qi, J., Cao, S., Biesiada, M., et al. 2019a, *PhRvD*, 100, 023530, doi: [10.1103/PhysRevD.100.023530](https://doi.org/10.1103/PhysRevD.100.023530)
- Qi, J.-Z., Cao, S., Zhang, S., et al. 2019b, *MNRAS*, 483, 1104, doi: [10.1093/mnras/sty3175](https://doi.org/10.1093/mnras/sty3175)

- Rana, A., Jain, D., Mahajan, S., & Mukherjee, A. 2017, JCAP, 2017, 028, doi: [10.1088/1475-7516/2017/03/028](https://doi.org/10.1088/1475-7516/2017/03/028)
- Räsänen, S., Bolejko, K., & Finoguenov, A. 2015, PhRvL, 115, 101301, doi: [10.1103/PhysRevLett.115.101301](https://doi.org/10.1103/PhysRevLett.115.101301)
- Ratra, B. 1994, PhRvD, 50, 5252, doi: [10.1103/PhysRevD.50.5252](https://doi.org/10.1103/PhysRevD.50.5252)
- Ratra, B., & Peebles, P. J. E. 1994, ApJL, 432, L5, doi: [10.1086/187498](https://doi.org/10.1086/187498)
- . 1995, PhRvD, 52, 1837, doi: [10.1103/PhysRevD.52.1837](https://doi.org/10.1103/PhysRevD.52.1837)
- Riess, A. G., Casertano, S., Yuan, W., et al. 2021, ApJL, 908, L6, doi: [10.3847/2041-8213/abdbaf](https://doi.org/10.3847/2041-8213/abdbaf)
- Ruan, C.-Z., Melia, F., Chen, Y., & Zhang, T.-J. 2019, ApJ, 881, 137, doi: [10.3847/1538-4357/ab2ed0](https://doi.org/10.3847/1538-4357/ab2ed0)
- Samushia, L., Dev, A., Jain, D., & Ratra, B. 2010, Physics Letters B, 693, 509, doi: [10.1016/j.physletb.2010.07.057](https://doi.org/10.1016/j.physletb.2010.07.057)
- Sapone, D., Majerotto, E., & Nesseris, S. 2014, PhRvD, 90, 023012, doi: [10.1103/PhysRevD.90.023012](https://doi.org/10.1103/PhysRevD.90.023012)
- Scolnic, D. M., Jones, D. O., Rest, A., et al. 2018, ApJ, 859, 101, doi: [10.3847/1538-4357/aab9bb](https://doi.org/10.3847/1538-4357/aab9bb)
- Shafieloo, A., & Clarkson, C. 2010, PhRvD, 81, 083537, doi: [10.1103/PhysRevD.81.083537](https://doi.org/10.1103/PhysRevD.81.083537)
- Shen, Y., Richards, G. T., Strauss, M. A., et al. 2011, ApJS, 194, 45, doi: [10.1088/0067-0049/194/2/45](https://doi.org/10.1088/0067-0049/194/2/45)
- Shen, Y., Wu, J., Jiang, L., et al. 2019, ApJ, 873, 35, doi: [10.3847/1538-4357/ab03d9](https://doi.org/10.3847/1538-4357/ab03d9)
- Simon, J., Verde, L., & Jimenez, R. 2005, PhRvD, 71, 123001, doi: [10.1103/PhysRevD.71.123001](https://doi.org/10.1103/PhysRevD.71.123001)
- Tegmark, M., Eisenstein, D. J., Strauss, M. A., et al. 2006, PhRvD, 74, 123507, doi: [10.1103/PhysRevD.74.123507](https://doi.org/10.1103/PhysRevD.74.123507)
- Trenti, M., Padoan, P., & Jimenez, R. 2015, ApJL, 808, L35, doi: [10.1088/2041-8205/808/2/L35](https://doi.org/10.1088/2041-8205/808/2/L35)
- Vagnozzi, S. 2020, PhRvD, 102, 023518, doi: [10.1103/PhysRevD.102.023518](https://doi.org/10.1103/PhysRevD.102.023518)
- . 2021, PhRvD, 104, 063524, doi: [10.1103/PhysRevD.104.063524](https://doi.org/10.1103/PhysRevD.104.063524)
- Vagnozzi, S., Loeb, A., & Moresco, M. 2021a, ApJ, 908, 84, doi: [10.3847/1538-4357/abd4df](https://doi.org/10.3847/1538-4357/abd4df)
- Vagnozzi, S., Pacucci, F., & Loeb, A. 2021b, arXiv e-prints, arXiv:2105.10421. <https://arxiv.org/abs/2105.10421>
- Valcin, D., Bernal, J. L., Jimenez, R., Verde, L., & Wandelt, B. D. 2020, JCAP, 2020, 002, doi: [10.1088/1475-7516/2020/12/002](https://doi.org/10.1088/1475-7516/2020/12/002)
- Verde, L., Treu, T., & Riess, A. G. 2019, Nature Astronomy, 3, 891, doi: [10.1038/s41550-019-0902-0](https://doi.org/10.1038/s41550-019-0902-0)
- Virey, J. M., Talon-Esmieu, D., Ealet, A., Taxil, P., & Tilquin, A. 2008, JCAP, 2008, 008, doi: [10.1088/1475-7516/2008/12/008](https://doi.org/10.1088/1475-7516/2008/12/008)
- Wang, B., Qi, J.-Z., Zhang, J.-F., & Zhang, X. 2020, ApJ, 898, 100, doi: [10.3847/1538-4357/ab9b22](https://doi.org/10.3847/1538-4357/ab9b22)
- Wang, F., Yang, J., Fan, X., et al. 2018, ApJL, 869, L9, doi: [10.3847/2041-8213/aaf1d2](https://doi.org/10.3847/2041-8213/aaf1d2)
- . 2021a, ApJL, 907, L1, doi: [10.3847/2041-8213/abd8c6](https://doi.org/10.3847/2041-8213/abd8c6)
- Wang, G.-J., Ma, X.-J., & Xia, J.-Q. 2021b, MNRAS, 501, 5714, doi: [10.1093/mnras/staa4044](https://doi.org/10.1093/mnras/staa4044)
- Wang, G.-J., Wei, J.-J., Li, Z.-X., Xia, J.-Q., & Zhu, Z.-H. 2017, ApJ, 847, 45, doi: [10.3847/1538-4357/aa8725](https://doi.org/10.3847/1538-4357/aa8725)
- Wei, J.-J. 2018, ApJ, 868, 29, doi: [10.3847/1538-4357/aae696](https://doi.org/10.3847/1538-4357/aae696)
- Wei, J.-J., & Melia, F. 2020a, ApJ, 897, 127, doi: [10.3847/1538-4357/ab959b](https://doi.org/10.3847/1538-4357/ab959b)
- . 2020b, ApJ, 888, 99, doi: [10.3847/1538-4357/ab5e7d](https://doi.org/10.3847/1538-4357/ab5e7d)
- Wei, J.-J., & Wu, X.-F. 2017, ApJ, 838, 160, doi: [10.3847/1538-4357/aa674b](https://doi.org/10.3847/1538-4357/aa674b)
- Wei, J.-J., Wu, X.-F., Melia, F., Wang, F.-Y., & Yu, H. 2015, AJ, 150, 35, doi: [10.1088/0004-6256/150/1/35](https://doi.org/10.1088/0004-6256/150/1/35)
- Witzemann, A., Bull, P., Clarkson, C., et al. 2018, MNRAS, 477, L122, doi: [10.1093/mnras/sly062](https://doi.org/10.1093/mnras/sly062)
- Wright, E. L. 2007, ApJ, 664, 633, doi: [10.1086/519274](https://doi.org/10.1086/519274)
- Xia, J.-Q., Yu, H., Wang, G.-J., et al. 2017, ApJ, 834, 75, doi: [10.3847/1538-4357/834/1/75](https://doi.org/10.3847/1538-4357/834/1/75)
- Yang, J., Wang, F., Fan, X., et al. 2019, AJ, 157, 236, doi: [10.3847/1538-3881/ab1be1](https://doi.org/10.3847/1538-3881/ab1be1)
- . 2020, ApJL, 897, L14, doi: [10.3847/2041-8213/ab9c26](https://doi.org/10.3847/2041-8213/ab9c26)
- Yang, Y., & Gong, Y. 2021, MNRAS, 504, 3092, doi: [10.1093/mnras/stab1085](https://doi.org/10.1093/mnras/stab1085)
- Yu, H., Ratra, B., & Wang, F.-Y. 2018, ApJ, 856, 3, doi: [10.3847/1538-4357/aab0a2](https://doi.org/10.3847/1538-4357/aab0a2)
- Yu, H., & Wang, F. Y. 2016, ApJ, 828, 85, doi: [10.3847/0004-637X/828/2/85](https://doi.org/10.3847/0004-637X/828/2/85)
- Zhao, G.-B., Xia, J.-Q., Li, H., et al. 2007, Physics Letters B, 648, 8, doi: [10.1016/j.physletb.2007.02.070](https://doi.org/10.1016/j.physletb.2007.02.070)
- Zheng, X., Cao, S., Liu, Y., et al. 2021, European Physical Journal C, 81, 14, doi: [10.1140/epjc/s10052-020-08796-w](https://doi.org/10.1140/epjc/s10052-020-08796-w)
- Zhou, H., & Li, Z. 2020, ApJ, 889, 186, doi: [10.3847/1538-4357/ab5f61](https://doi.org/10.3847/1538-4357/ab5f61)